



Black carbon enrichment in atmospheric ice particle residuals observed in lower tropospheric mixed phase clouds

J. Cozic,^{1,2} S. Mertes,³ B. Verheggen,^{1,4} D. J. Cziczo,^{5,6} S. J. Gallavardin,⁵ S. Walter,⁷ U. Baltensperger,¹ and E. Weingartner¹

Received 10 August 2007; revised 25 February 2008; accepted 1 April 2008; published 15 August 2008.

[1] The enrichment of black carbon (BC) mass in residuals of small ice crystals was investigated during intensive experiments in winter 2004 and 2005 at the high alpine research station Jungfraujoch (3580 m asl, Switzerland). Two inlets were used to sample the bulk aerosol (residuals of cloud droplets and ice crystals and nonactivated aerosol particles) and the residual particles of small ice crystals (diameter 5–20 μm). An enrichment of the BC mass fraction in the ice particle residuals was observed by investigating the measured BC mass concentration as a fraction of the bulk (submicrometer) aerosol mass concentration sampled by the two inlets. On the average, the BC mass fraction was 5% for the bulk aerosol but 27% for the ice particle residuals. The observed enrichment of BC in ice particle residuals suggests that some BC-containing particles may preferentially act as ice nuclei, with important implications for the indirect aerosol effect via glaciation of clouds if these particles represent a significant fraction of the number of ice crystals nucleated.

Citation: Cozic, J., S. Mertes, B. Verheggen, D. J. Cziczo, S. J. Gallavardin, S. Walter, U. Baltensperger, and E. Weingartner (2008), Black carbon enrichment in atmospheric ice particle residuals observed in lower tropospheric mixed phase clouds, *J. Geophys. Res.*, 113, D15209, doi:10.1029/2007JD009266.

1. Introduction

[2] The ability of aerosol particles to act as cloud condensation nuclei (CCN) or ice nuclei (IN) influences the optical properties and lifetime of clouds. The resulting aerosol indirect effect has been recognized as the greatest source of uncertainty in assessing human impact on climate [IPCC, 2007]. The properties of clouds and their formation processes are poorly understood, particularly those of mixed phase and ice clouds [Penner *et al.*, 2001]. Increased IN concentrations are thought to enhance precipitation, thus causing a decrease in cloud lifetime and cloud cover, resulting in a warming of the atmosphere [Lohmann, 2002; Lohmann and Diehl, 2006]. This would act in the opposite direction compared to the indirect effect of aerosols acting as CCN in liquid or mixed phase clouds.

[3] Black carbon (BC) is formed by combustion processes and is an important aerosol component in the Earth's troposphere [Finlayson-Pitts and Pitts, 2000; Heintzenberg, 1989; Seinfeld and Pandis, 1998]. BC has many sources and is likely dominated by anthropogenic emissions. Because of the variety of sources, BC is a complicated aerosol system. It can be associated with many different components, depending on how and where it was produced. Ice core measurements show that BC concentrations in the atmosphere have increased from preindustrial to modern times [Lavanchy *et al.*, 1999]. The ability of BC containing particles to act as IN has gathered interest and it has been investigated since increasing concentrations of an anthropogenic IN component would have a strong impact on cloud properties.

[4] To date, the ability of different aerosols to act as IN has predominantly been studied in laboratory experiments. A number of nucleation modes are known to form ice, and these include the direct deposition of water vapor (deposition), from within a droplet (immersion), and upon contact with a droplet (contact) [Pruppacher and Klett, 1997]. It has been found that IN are generally insoluble particles, such as certain types of mineral dusts and metallic particles [see DeMott, 2002, and references therein]. The ability of BC to act as IN has also been investigated in different laboratory studies [DeMott, 1990; DeMott *et al.*, 1999; Diehl and Mitra, 1998; Dymarska *et al.*, 2006; Gorbunov *et al.*, 2001; Möhler *et al.*, 2005a, 2005b]. These studies include BC aerosols produced by a number of methods from dry dispersions of powders to flame-generated soot. The role of coatings, for example organic materials and sulfuric acid,

¹Laboratory of Atmospheric Chemistry, Paul Scherrer Institut, Villigen PSI, Switzerland.

²Now at NOAA, Earth System Research Laboratory, Boulder, Colorado, USA.

³Leibniz Institute for Tropospheric Research, Leipzig, Germany.

⁴Now at Department of Air Quality and Climate Change, Energy Research Centre of the Netherlands ECN, Petten, Netherlands.

⁵Institute for Atmospheric and Climate Science, ETH Zürich, Zürich, Switzerland.

⁶Now at Pacific Northwest National Laboratory, Atmospheric Science and Global Change Division, Richland, Washington, USA.

⁷Particle Chemistry Department, Max Planck Institute for Chemistry, Mainz, Germany.

was examined. In general, these studies are most surprising in that they find no consensus as to the nucleating ability of BC. For example, *Gorbunov et al.* [2001] found that oxidized soot particles can form ice crystals effectively and they suggested that chemical groups on the oxidized surface can form hydrogen bonds with water molecules which can contribute to the formation of ice. It is not clear what freezing mechanisms were in play during this study, however. Likewise, *Diehl and Mitra* [1998] returned relatively high freezing thresholds for all nucleation modes with immersion ice nucleation by BC particularly effective, with nucleation up to -20°C . By contrast most other researchers have found that BC is a relatively poor IN. Most studies have shown onset of ice nucleation not occurring above -25°C nor much below water saturation.

[5] Ice particle residual composition (thought to be representative of IN) has been characterized in a number of field studies. These include some from aircraft platforms [*Chen et al.*, 1998; *Cziczo et al.*, 2004; *Heintzenberg et al.*, 1996; *Prenni et al.*, 2007; *Rogers et al.*, 2001; *Targino et al.*, 2006; *Twohy and Poellot*, 2005], including data in contrails [*DeMott et al.*, 2003; *Schröder et al.*, 1998; *Ström and Ohlsson*, 1998a, 1998b], and at high-altitude mountain-top sites using diffusional growth chambers [*DeMott et al.*, 2003; *Richardson et al.*, 2007]. As it has been the case for laboratory studies, no clear consensus as to the role of BC in ice nucleation has been reached in the field studies. For example, BC was found in contrail ice but it is not clear if nucleation or scavenging was responsible [*Kärcher et al.*, 2007; *Ström and Ohlsson*, 1998a, 1998b]. In some studies enhanced levels of carbonaceous particles were found in ice residue [e.g., *Chen et al.*, 1998] whereas in others virtually no BC-like material was detected in cirrus ice [*Cziczo et al.*, 2004].

[6] The partitioning of BC in lower tropospheric mixed phase clouds was investigated by *Cozic et al.* [2007]. It was found that in liquid clouds about 60% of the BC mass was incorporated into the cloud phase by nucleation scavenging. BC was found to be scavenged into the condensed phase to the same extent as the bulk aerosol [*Cozic et al.*, 2007; *Verheggen et al.*, 2007]. This was caused by the high degree of internal mixing (also shown by hygroscopicity measurements [*Sjogren et al.*, 2007]), i.e., the BC particles were coated with a large amount of soluble material which was responsible for the particle activation into cloud droplets. In mixed phase clouds BC was also found to be scavenged to the same extent as the bulk aerosol but under these conditions the scavenged fractions were considerably lower (around 10%) because in the presence of ice the droplets evaporate and the scavenged BC mass is released back into the interstitial aerosol. (It is also possible that less droplets were formed in the presence of ice.) This points to the importance of the ice crystals which are much less numerous than cloud droplets in mixed phase clouds (typically 1%). Here we go a step further by using another inlet which enabled the extraction of ice particle residuals in mixed phase clouds and allowed us to characterize only the small ice residuals at the origin of ice formation.

[7] In this work we will compare the mass fraction of BC in ice particle residuals (in the following denoted as ice residuals) with the BC fraction of the bulk aerosol. These fractions were determined during approximately 140 hours

of in-cloud measurements in lower tropospheric clouds at the high alpine site Jungfraujoch. This mass based chemical characterization of IN is clearly valuable, however, even more important is chemical information in terms of number because the number of IN has a stronger influence on cloud microphysics than their mass. Therefore the data on the BC mass fractions are complemented with data obtained with a single particle mass spectrometer (ATOFMS) which was operated during a shorter time period to derive number-based chemical information of the ice residuals.

2. Experimental

[8] Measurements were conducted during three *Cloud and Aerosol Characterization Experiments* (CLACE) at the high-alpine research station Jungfraujoch (Switzerland, 3580m asl.). CLACE campaigns aimed at characterizing the physical and chemical properties of aerosol particles in general and of CCN and IN [*Cozic et al.*, 2008; *Mertes et al.*, 2007], and at quantifying the partitioning of aerosol in mixed phase clouds [*Cozic et al.*, 2007; *Verheggen et al.*, 2007].

[9] Sampling was carried out in March 2004 (CLACE 3), from mid February to mid March 2005 (CLACE 4). Approximately 140 hours of data in mixed phase clouds with temperatures (with the sampling location being within the cloud) ranging from -28 to -5°C were collected. Although clouds were predominantly convective, an orographic effect at the Jungfraujoch region is always present. Moreover, there exists no information about cloud base and cloud top and where inside the cloud the sampling took place. However, these are not the key parameters for this study. According to the usual ice particle growth rate, the investigated small ice particles most likely formed close to the sampling point, which means that the local microphysical cloud parameters and temperature are most important. Physical and chemical aerosol parameters were simultaneously measured downstream of several different inlets as described below.

2.1. Jungfraujoch Station

[10] The Jungfraujoch measurement site is located on an exposed mountain saddle in the Swiss Alps at 3580 m asl. The site is deemed representative of the mid-European lower free troposphere and is a Global Atmosphere Watch (GAW) station where atmospheric aerosols and gases have been measured for over a decade. The station is regularly engulfed in clouds (30% of the time averaged over the two campaigns). Due to its location and altitude, the site is far from significant pollution sources. These characteristics make the Jungfraujoch well suited to investigate continental background aerosols and clouds from a ground based platform. More information on the Jungfraujoch site and the long-term aerosol measurements are given by *Baltensperger et al.* [1997] and *Collaud Coen et al.* [2007].

2.2. Inlets

[11] The partitioning of aerosol particles in mixed phase clouds was investigated by sampling air through various inlets. A heated (25°C) total inlet was used to sample all cloud droplets and ice crystals smaller than $40\ \mu\text{m}$ at wind speeds of up to $20\ \text{m s}^{-1}$ and to evaporate them at an early

stage of the sampling process [Weingartner *et al.*, 1999]. This total inlet thus samples the bulk aerosol which consists of aerosol particles incorporated into cloud droplets and ice crystals and of interstitial (nonactivated) particles. This inlet is also used for the continuous GAW measurements.

[12] Another inlet, the Ice Counterflow Virtual Impactor (Ice-CVI), was designed to sample only small ice crystals in the diameter range 5–20 μm [Mertes *et al.*, 2007]. Ice crystals up to 20 μm only grow by water vapor diffusion and are not significantly affected by riming [Chen and Lamb, 1999; Fukuta and Takahashi, 1999] or particle scavenging. Song and Lamb [1994] estimated the number of scavenged interstitial particles per ice particle and observed particle scavenging for ice crystals between 60 and 200 μm in diameter, which is significantly larger than the Ice-CVI sampling size range. Such calculations were performed for the Jungfraujoch conditions considering an upper limit of 1000 cm^{-3} for the interstitial particle concentration at the Jungfraujoch yielding some tenth of a percent scavenged particles by one sampled ice particle. This clearly shows that particle impaction scavenging is negligible in the context of this study. This conclusion is also supported by measurements of ice particle and ice particle residual concentrations with a Cloud Particle Imager and the Ice-CVI [Mertes *et al.*, 2007] which agreed within 40%. We therefore assume that the extracted ice particle residuals are representative of IN. The first stage of the Ice-CVI consists of a virtual impactor, which removes hydrometeors larger than 20 μm in diameter. Then, an inertial preimpactor removes the supercooled droplets as they freeze upon impaction on plates held below -5°C . Small ice crystals are expected to bounce off and be carried with the sample air stream, as verified experimentally by Tenberken Pötzsch *et al.* [2000]. Finally, aerosol particles that bounce and have diameters below 5 μm are removed by a Counterflow Virtual Impactor, whereas the larger ice crystals (diameters between 5 and 20 μm) overcome the counterflow. Downstream of the Ice-CVI inlet the condensed water of the ice crystals is completely sublimated in a particle free, dry carrier gas. In this manner dry residual aerosol particles can be subsequently analyzed. The Ice-CVI inlet can also run without impactors and without counterflow (i.e., sampling the bulk aerosol under cloud-free conditions). More details on the Ice-CVI design, operation and results are described by Mertes *et al.* [2007].

[13] Possible sampling artefacts of the Ice-CVI are extensively discussed in Mertes *et al.* [2007] with respect to deposition losses, ice particle break up, particles abrasion from the inner inlet surfaces and presegregation of supercooled drops. The restriction of the upper sampling size limit to 20 μm by means of a 90° sampling inlet and a virtual impactor, avoids breakup of large ice crystals inside the Ice-CVI. The remaining small ice particles do not easily shatter inside the system due to the low sampling air velocities; this is in contrast to airborne measurements. High air velocities persist only in the wind tunnel in front of and shortly behind the CVI tip. However, due to the vertical Ice-CVI setup there are no opposing surfaces where particle breakup or abrasion could easily occur. Lab tests and field measurement clearly demonstrated the successful segregation of supercooled drops.

[14] The CVI sampling principle leads to an enrichment of the collected hydrometeors (and thus of the residual particles), which is essential for the determination of the expected low IN number and mass concentration. The enrichment is given by the velocity ratio upstream and downstream the Ice-CVI inlet tip [see details in Mertes *et al.*, 2007]. Enrichment factors between 5 and 10 were reached with our sampling and detection configuration.

2.3. Black Carbon Measurements

[15] Two Particle Soot Absorption Photometers (PSAP, Radiance Research) [Reid *et al.*, 1998] were used to measure the particle light absorption coefficient at a defined wavelength ($\lambda = 580 \text{ nm}$) downstream of the total inlet and Ice-CVI, respectively. The primary measure of the PSAP (light attenuation coefficient, b_{ATN}) was converted into an absorption coefficient (b_{abs}) by using the method described by Bond *et al.* [1999]. No scattering coefficient correction was applied ($b_s = 0$), because the aerosol light scattering coefficient was measured downstream of the total inlet only. Analyzing the data behind the total inlet showed that neglecting the scattering coefficient tends to overestimate the BC concentration by 17% on average. The aerosol absorption coefficient b_{abs} at a wavelength $\lambda = 580 \text{ nm}$ was converted to a BC mass concentration by dividing b_{abs} by a mass absorption efficiency $\sigma_{abs,BC}$ of $8.5 \text{ m}^2 \text{ g}^{-1}$ [Bond and Bergstrom, 2006; Cozic *et al.*, 2008].

2.4. Particle Size Distribution Measurements

[16] Two Scanning Mobility Particle Sizers (SMPS, TSI 3934), comprising a Differential Mobility Analyzer (DMA, TSI 3071) and a Condensation Particle Counter (CPC, TSI 3022), were used to measure the particle size distribution between 17 and 900 nm (dry) diameter [Verheggen *et al.*, 2007]. One SMPS was operated at the total inlet whereas another one was dedicated to the Ice-CVI inlet.

[17] These instruments were complemented by two optical particle counters (OPC, Grimm Dustmonitor 1.108) measuring the particle size distribution in the diameter range of 0.3 to 20 μm behind both inlets. The factory calibration of the OPC with LATEX spheres was used and the correct sizing of the OPCs and SMPS was checked with monodisperse LATEX spheres in the laboratory and during the experiment.

[18] The measured SMPS size distributions were used to derive the bulk submicrometer volume of particles sampled downstream of each inlet ($V_{SMPS(\text{Total})}$ and $V_{SMPS(\text{Ice-CVI})}$) assuming a spherical particle shape. In the same manner combined volume concentrations ($V_{SMPS+OPC}$) were calculated using the SMPS (mobility diameter $d = 17\text{--}900 \text{ nm}$) and the OPC measurements (limited to $d = 0.9\text{--}20 \mu\text{m}$).

[19] Validation of the SMPS measurements was performed by comparing the derived aerosol number concentration from the SMPS with the aerosol number concentration measured directly with two additional CPCs (TSI 3010) placed behind the total and the Ice-CVI inlet.

2.5. Aerosol Mass Spectrometry

[20] An Aerodyne quadrupole aerosol mass spectrometer (Q-AMS, Jayne *et al.* [2000]) was used for measuring online chemically resolved submicrometer mass concentrations of nonrefractory aerosol components (sulfate, nitrate,

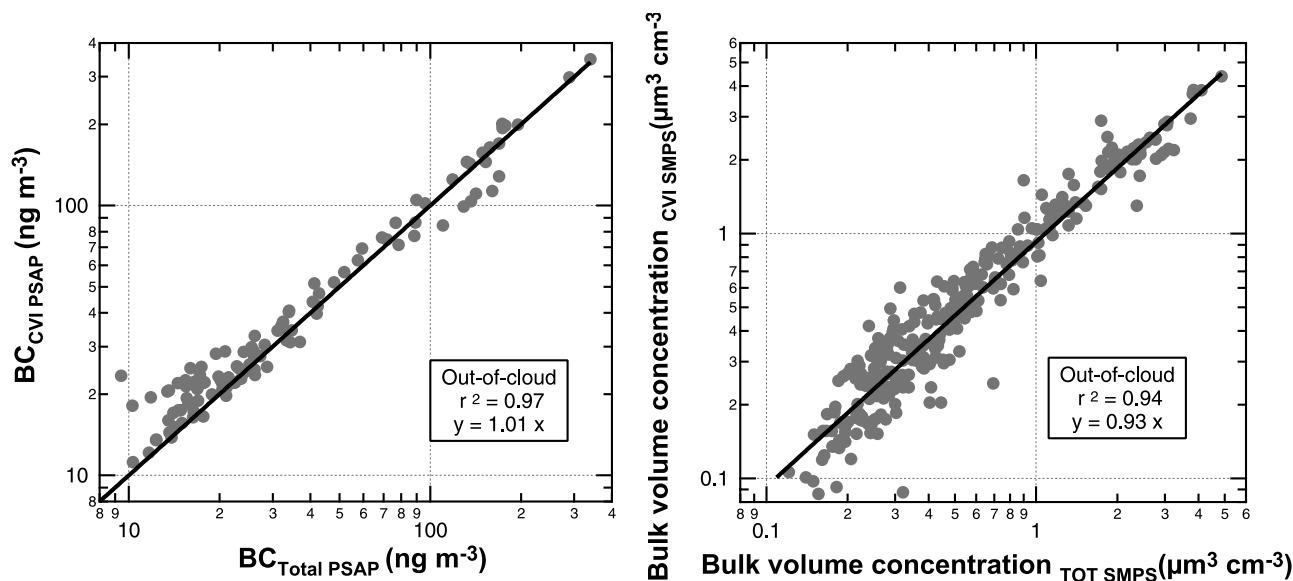


Figure 1. Comparison of the (a) PSAP (117 hours) and (b) SMPS (328 hours) measuring downstream of the two different inlets in clear sky conditions ($LWC < 0.01 \text{ g m}^{-3}$), where the Ice-CVI was operated as a regular inlet. Symbols represent 1-hour averages. Data are presented on logarithmic scales.

ammonium, organics). The instrument was measuring ice residuals in-cloud and bulk aerosol out of cloud.

2.6. Single-Particle Aerosol Mass Spectrometry

[21] An Aerosol Time of Flight Mass Spectrometry (ATOFMS; TSI Model 3800) was deployed during an additional campaign from mid February to mid March 2006 and was switched between the total and Ice-CVI inlet. The ATOFMS operates by drawing a flow of 100 sccm into a vacuum. This flow passes through an aerodynamic lens which is used to focus particles into the beampath of two continuous 532-nm lasers. The transit time between the two beams is used to size particles and to trigger a 266-nm pulsed laser. The 266-nm laser is used to desorb and ionize components. The wavelength is sufficient to ablate most typical atmospheric aerosol components, from volatile to refractory. Both negative and positive polarity ions are detected using dual reflectron mass spectrometers and this provides a qualitative understanding of chemical composition on the single particle level [Gard *et al.*, 1997].

[22] The smallest particles detected using the ATOFMS during this deployment were $\sim 200 \text{ nm}$ and the largest $\sim 2000 \text{ nm}$ in aerodynamic diameter. Transmission at the limits does not behave as a step function; instead, there is a nonmonotonic decrease as these limits are approached [Liu *et al.*, 2007]. It is also known that transmission through an aerodynamics lens is a complex function of particle size, shape, and phase [e.g., Zelenyuk *et al.*, 2006]. Black carbon and other highly fractal material is not transmitted as efficiently as spherical particles. Because of this, and because atmospheric particles containing black carbon normally lie toward the lower end of this transmission range, these data should be considered a lower limit for their number.

2.7. Cloud Microphysical Measurements

[23] Cloud liquid water content (LWC) was measured with a Particulate Volume Monitor (PVM-100, Gerber

Scientific) with 1 minute time resolution. The instrument response was typically calibrated every cloud-free day. The response of the PVM was corrected for the presence of ice [see Verheggen *et al.*, 2007] but was only used as cloud marker in this study.

[24] In the following analysis, a 1-hour time interval was classified as being “in-cloud” when the 15th percentile of the Liquid Water Content (LWC) was larger than 0.02 g m^{-3} and the average $LWC > 0.05 \text{ g m}^{-3}$. This criterion was chosen to ascertain that measurements made in cloud edges, patchy clouds, and regions influenced by strong entrainment effects are excluded from the analysis.

3. Results and Discussion

3.1. Comparison of Identical BC and Aerosol Volume Instruments Behind the Two Inlets

[25] The analysis of the enrichment of BC in the ice phase requires an assessment of possible artifacts induced by the sampling procedures at each inlet. Under clear sky conditions (periods for which the average LWC during 1 hour was below 0.01 g m^{-3}), the proper functioning of the two PSAP and SMPS instruments was evaluated. This was done by comparing the PSAP BC mass concentrations and SMPS aerosol volume concentrations measured downstream of the total inlet and the Ice-CVI inlet without impactors and without counterflow (i.e., sampling the bulk aerosol under cloud-free conditions).

[26] Figure 1 shows that the BC mass concentrations from the two PSAPs are in good agreement ($r^2 = 0.97$; $BC_{\text{PSAP(Ice-CVI)}} = 1.01 \cdot BC_{\text{PSAP(Total)}}$). The BC concentrations at the Ice-CVI inlet were slightly higher than those at the total inlet. In order to provide the best evaluation of the BC enrichment, the Ice-CVI PSAP data were corrected for this small deviation which could be explained from differences in different sampling line losses and/or instrument performance (differences in flow calibration, PSAP spot size). This comparison and correction was also done for the particle

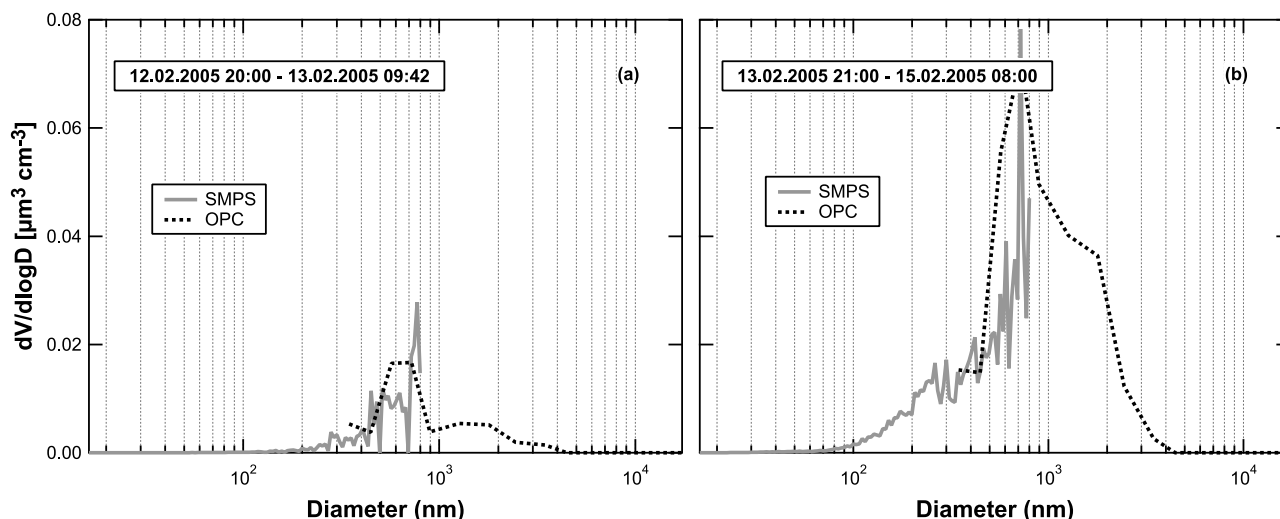


Figure 2. Volume size distributions of ice residuals during a cloud derived from SMPS and OPC for the period 12–15 February 2005.

volume derived from the two SMPS systems which also showed a good agreement ($r^2 = 0.94$; $V_{\text{SMPS}(\text{Ice-CVI})} = 0.93 \cdot V_{\text{SMPS}(\text{Total})}$).

3.2. Ice Residual Characteristics

[27] The ice particle residual and bulk aerosol chemical composition of the nonrefractory components in the submicrometer size range were measured with an aerosol mass spectrometer and compared to the SMPS derived mass given by $V_{\text{SMPS}(\text{Total})} \cdot \rho_{(\text{Bulk})}$ and $V_{\text{SMPS}(\text{Ice-CVI})} \cdot \rho_{(\text{Ice residuals})}$, where ρ is the average particle density. From the measured chemical composition of the submicrometer bulk aerosol [Cozic *et al.*, 2008] a density $\rho_{(\text{Bulk})} = 1.5 \text{ g cm}^{-3}$ was estimated (mixture of organics ($\rho = 1.2 \text{ g cm}^{-3}$), ammonium sulfate ($\rho = 1.77 \text{ g cm}^{-3}$) and ammonium nitrate ($\rho = 1.7 \text{ g cm}^{-3}$)). Ice particle residuals were assumed to be a mixture of mineral dust ($\rho = 2.5 \text{ g cm}^{-3}$, [Linke *et al.*, 2006]), soluble material ($\rho = 1.5 \text{ g cm}^{-3}$) and BC ($\rho = 2 \text{ g cm}^{-3}$, [see Fuller *et al.*, 1999, and references therein]) so that a value of 2 g cm^{-3} was chosen for $\rho_{(\text{Ice residuals})}$. The comparison of AMS and SMPS derived submicrometer mass concentrations showed that the chemical composition of ice residuals was remarkably different from the bulk aerosol [Walter *et al.*, Chemical composition measurements of ice nuclei in mixed phase tropospheric clouds during the Cloud and Aerosol Characterization Experiments CLACE, in preparation]. This comparison confirms the findings of Krivacsy *et al.* [2001] and Cozic *et al.* [2008] that the submicrometer bulk aerosol is dominated by nonrefractory material (sulfate, nitrate, ammonium, and organics).

[28] Ice residuals showed a significantly different signature. Ice crystal residuals from the Ice-CVI measured by the AMS showed a negligible mass concentration compared to the SMPS derived mass. This alone is suggestive that refractory particles (such as mineral dust and BC) preferably act as IN [Mertes *et al.*, 2007]. In the following, we attempt to quantify the relative amount of BC in ice residuals which allow us to study the enrichment of BC in the ice residual phase compared to the bulk aerosol.

[29] Typical SMPS and OPC volume size distributions of ice residuals are presented in Figure 2 during a mixed phase

cloud in the period 12–14 February 2005. The measured volume size distributions often showed some bimodal structure. For clarity, the data during this cloud event are split into two periods. In the first period (Figure 2a) a first mode appeared at $d = \sim 600 \text{ nm}$, and no strong influence from supermicrometer sized particles (second mode) was observed. During the second period (Figure 2b) the relative amount of the latter particles strongly increased and this second mode clearly extended into the submicrometer size range. It is hypothesized that the first mode consisted mainly of BC containing particles while the second mode was composed of mineral dust. This is supported by Cozic *et al.* [2007] who showed by comparison of two BC instruments (one measuring TSP and the other one measuring PM₂) that BC particles were predominantly found in the fine mode ($d < 1 \mu\text{m}$).

[30] In addition, BC in the ice residues was also detected with the ATOFMS running during an additional campaign in February–March 2006. Figure 3 presents the normalized number of particles as a function of aerodynamic diameter. Particles are binned in 0.1-micrometer diameter increments. The solid black line is the total number of particles for which chemical composition was determined. The dotted line is the subset of black carbon containing particles (i.e., those which exhibited C_n features where C is mass 12 and n is an integer). The dashed line is the subset of particles which had features associated with mineral dust (e.g., iron, aluminum, silicon, etc.). Panel (a) shows data for particles sampled from the total inlet. Panel (b) shows data for particles sampled from the Ice-CVI. The BC ice residual size distribution during this campaign was centered at 350 nm (first mode), slightly smaller than the 450 nm size of the bulk aerosol measured from the total inlet. As previously mentioned, the highly fractal particles and those smaller or larger than the range to which the ATOFMS is sensitive would be undercounted by this instrument. The second mode is attributed to mineral dust particles as confirmed by single particle analysis with electron microscopy of IN samples that were collected downstream of the Ice-CVI [Mertes *et al.*, 2007].

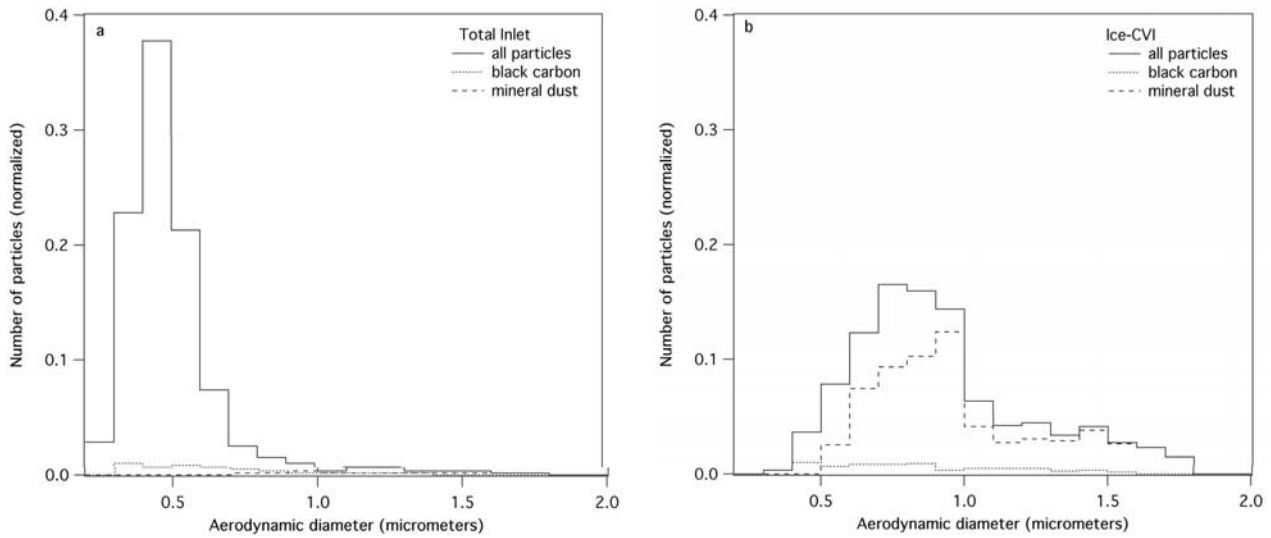


Figure 3. Normalized number of particles (total number of particles for which chemical composition was determined, subset of black carbon, subset of particles which had features associated with mineral dust (e.g., iron, aluminum, silicon, etc)) as a function of aerodynamic diameter analyzed by the ATOFMS during February–March 2006 for sample (a) from the total inlet and (b) from ice residuals. Particles are binned in 0.1-micrometer diameter increments. Note that the data is not corrected for the ATOFMS detection efficiency, which is low at the lower end of the reported size range where the BC containing particles are expected.

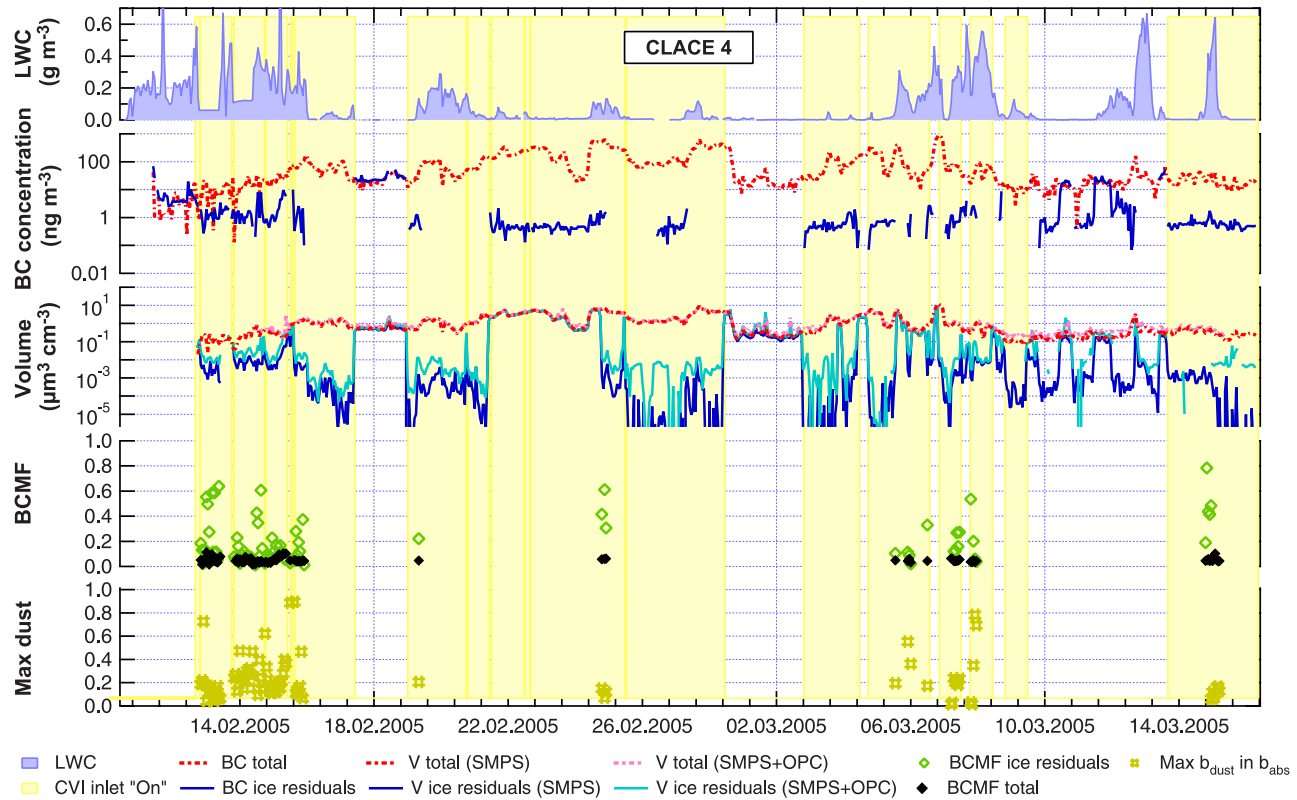


Figure 4. Time series of the BC and aerosol volume concentrations behind the total and the Ice-CVI inlet for the winter campaign in 2005 on logarithmic concentration scales. The BC mass fractions (*BCMF*) of the ice residuals and bulk particles, as well as the maximum contribution of mineral dust to the measured absorption (expressed as a fraction) are also presented (*max dust*). The presence of clouds is seen in higher liquid water content (*LWC*) values, and the periods where the Ice-CVI was extracting ice residuals are visualized with yellow bands. All data are presented as 1-hour averages.

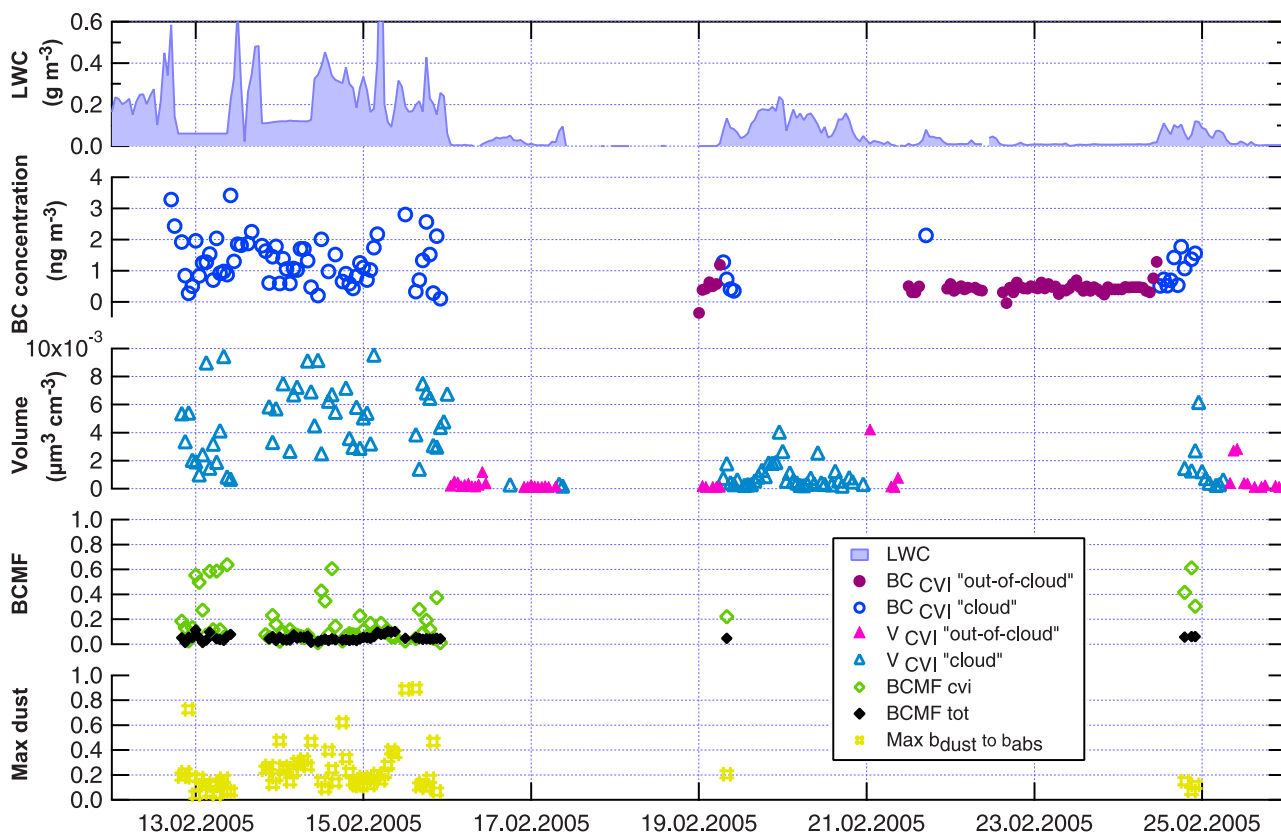


Figure 5. Time series of the liquid water content (LWC), BC concentration, aerosol volume concentration, and BC mass fraction ($BCMF$) behind the CVI and the total inlet as well as the estimated maximum contribution of mineral dust to the measured absorption (max dust). During the cloudy nights of 13 and 14 February, the PVM was clogged with snow, which is recognizable in two periods with relatively constant PVM signals. During these periods the LWC measurements are expected to be underestimated. All data are presented as 1-hour averages.

[31] In the following, the presence of BC in submicrometer ice residuals, their concentration and enrichment in the ice phase compared to the bulk aerosol are presented.

3.3. Time Series of BC and Aerosol Volume Behind the Ice-CVI

[32] Figure 4 (top) presents a time series of the liquid water content (LWC) which indicates the presence of cloud during the field campaign of February–March 2005. The next two regions in Figure 4 show the temporal evolution of the BC and aerosol submicrometer volume concentrations measured behind the total and Ice-CVI inlets. Within clouds the measured concentrations behind the Ice-CVI inlet (in blue) were a factor of 10 to 100 lower than behind the total inlet (in red). The respective concentrations were similar when the Ice-CVI inlet was running as a regular inlet during clear-sky conditions (for example on 17–18 February 2005). Similar evolutions of BC and particle volume concentrations were also observed in March 2004.

[33] Besides BC, mineral dust also absorbs visible light. In order to assess an upper limit for the contribution of mineral dust to the measured absorption downstream of the Ice-CVI the maximum absorption from mineral dust was estimated by assuming that the entire particle mass behind the Ice-CVI consisted of mineral dust. A maximum mineral dust mass concentration was calculated from combined number size

distributions measurements of the SMPS ($d = 17–900$ nm) and the OPC ($d = 0.9–20$ μm) ($V_{SMPS+OPC(Ice-CVI)}$) assuming that the complete ice residual mass consisted of mineral dust with a density of 2.5 g cm⁻³ [Linke *et al.*, 2006] and that particles were spherical. This mass concentration was then converted into an absorption coefficient $b_{abs(mineral\ dust)}$ by using an upper limit for the mineral dust mass absorption efficiency of 0.04 m²g⁻¹ at $\lambda = 580$ nm. This value was derived from the maximum dust mass absorption efficiency of 0.02 m²g⁻¹ at 660 nm, measured by Alfaro *et al.* [2004] and Linke *et al.* [2006] and converted to 580 nm by estimating a factor of two from the refractive index modeling of Sokolik and Toon [1999], who found a decrease of the imaginary part with increasing wavelength. The ratio of $b_{abs(mineral\ dust)}$ to the measured absorption coefficient is thus a measure for the upper limit of the mineral dust contribution to the measured absorption (max dust). This ratio is included in Figure 4 and Figure 5 and it is seen that on average the maximum contribution of mineral dust to the absorption was 15%. Figure 4 also presents the temporal evolution of the BC mass fraction in the bulk aerosol and in the ice residuals, which will be discussed in section 3.4.

[34] Figure 5 shows in more detail the temporal evolution of the same parameters on linear concentration scales for the

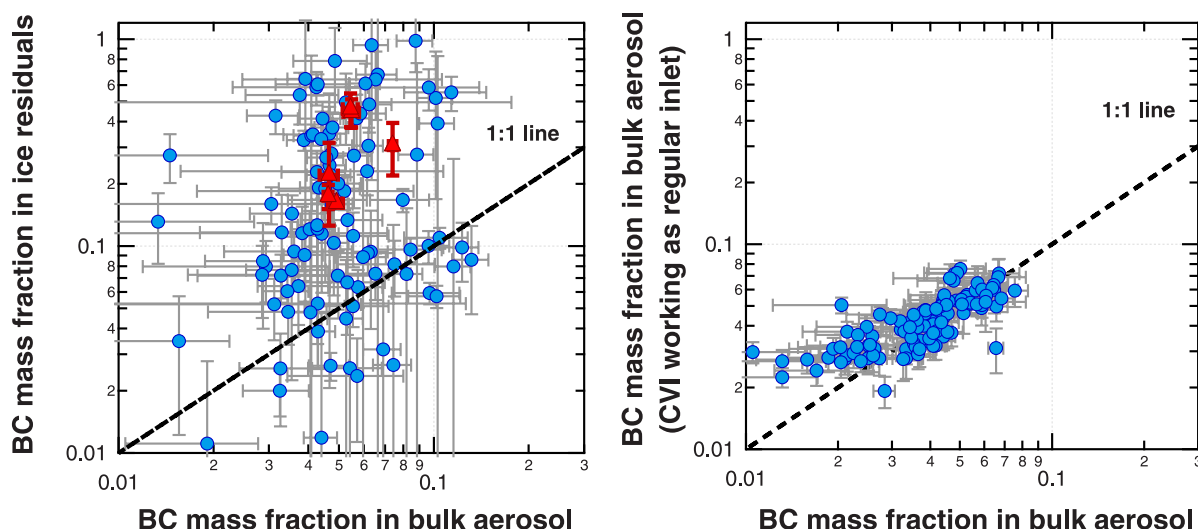


Figure 6. Comparison of the BC mass fraction in the ice particle residual phase with the corresponding fraction in the bulk aerosol phase (a) in cloud (106 hours) and (b) out of cloud (Ice-CVI operated as a regular inlet) (113 hours). Blue circles represent hourly averaged data, whereas triangular red points present averages over six individual cloud periods. Their corresponding errors are also plotted. Note that the scales are logarithmic.

period 12–17 February 2005. For this period about 60 hours of in-cloud data with all instruments running are available. The BC concentrations in ice residuals were relatively low: Between February 12 and 15 concentrations were $1.3 \pm 0.8 \text{ ng m}^{-3}$ on average, with a maximum of 3.8 ng m^{-3} . The corresponding average BC concentration of the bulk aerosol was 22.5 ng m^{-3} . As previously explained, both values (behind the total and the Ice-CVI inlets) are expected to be slightly overestimated due to the missing scattering correction. This bias was estimated to be $<20\%$ for the measurements behind the total inlet.

[35] It can be seen in Figure 5 that the BC concentrations measured downstream of the Ice-CVI inlet were significantly higher during the presence of clouds (dark blue dots) compared to out-of-cloud (dark purple dots) periods (average 0.4 ng m^{-3}). Out of cloud, when the CVI was running, virtually no particles were detected with the CPC, SMPS and OPC (number concentration $< 0.01 \text{ cm}^{-3}$; volume concentration $< 10^{-4} \mu\text{m}^3 \text{ cm}^{-3}$). The value of $0.4 \pm 0.1 \text{ ng m}^{-3}$ was thus not caused by a leak in the CVI sampling lines and has to be attributed to an instrumental offset of the PSAP. It was not possible to find a specific reason for this offset and since we do not know if it was also present at higher-measured concentrations, this offset was not subtracted from the measured BC concentrations. However, an analysis showed that a subtraction of this offset would not significantly change the results (see below).

3.4. BC Mass Fractions in the Bulk Aerosol and in Ice Residuals

[36] The BC mass fractions ($BCMF$) of the submicrometer aerosol downstream of the total inlet ($BC_{\text{PSAP(Total)}} / (V_{\text{SMPS(Total)}} \cdot \rho_{\text{(Bulk)}})$) and of the Ice-CVI ($BC_{\text{PSAP(Ice-CVI)}} / (V_{\text{SMPS(Ice-CVI)}} \cdot \rho_{\text{(Ice residuals)}})$), were studied during two field campaigns in March 2004 and February–March 2005, where BC and volume concentrations were obtained from

the respective PSAP and SMPS measurements. Densities of 1.5 g cm^{-3} for the bulk aerosol and 2 g cm^{-3} for ice residuals were used as previously explained. The calculated $BCMF$ describe a property of the aerosol and are not dependent on specific characteristics of the inlets (e.g., CVI collection efficiency, enrichment factor, etc.).

[37] The time series of the $BCMF$ in the ice residuals and in the bulk aerosol are presented for February–March 2005 in Figure 4 and for a typical case in Figure 5. It can be observed that the $BCMF$ in the bulk aerosol (solid points) was relatively constant at around 5% on average, but the $BCMF$ in the ice residuals (green points) was more variable, ranging from 12 to 38% (given as average values for different cloud periods when the cloud event was longer than 3 hours). Averaged over all cloud events, the $BCMF$ in the ice residuals was about 27% compared to 5% in the bulk aerosol. Identical results of the $BCMF$ in the bulk aerosol were previously shown in a mass closure study at Jungfraujoch [Cozic et al., 2008]. The value of 27% would be lowered to 16% if the observed BC concentration offset was subtracted from the measured concentrations.

[38] Figure 6a compares the $BCMF$ in the ice residuals with those in the bulk aerosol for all data where simultaneously measured BC mass fractions were available (totally 106 hours of in-cloud data). Blue circles represent individual hourly averaged data whereas triangular red points represent averaged $BCMF$ over 6 individual cloud events. In addition, their corresponding errors were added. To estimate the error of the BC concentrations, a detection limit of the PSAP of $DL \sim 0.3 \text{ ng m}^{-3}$ (for 1-hour averages, considering the CVI enrichment factor) and $DL \sim 3 \text{ ng m}^{-3}$ (for 1-hour averages behind the total inlet) were used. For the SMPS measurements, additional uncertainties were introduced by the conversion of aerosol number into aerosol mass assuming a certain density, and by the uncertainty in the aerosol size distribution measurements (estimated to

10% of the measured volume). The errors on the $BCMF$ were estimated as

$$\Delta BCMF = BCMF \cdot \sqrt{\frac{(\Delta BC)^2}{BC^2} + \frac{(\Delta V)^2}{V^2}} \quad (1)$$

with

$$\Delta BC = \sqrt{(DL)^2 + (0.05 \cdot BC)^2} \text{ and } \Delta V = 0.10 \cdot V.$$

[39] Figure 6a yields information on the enrichment of BC in the ice particle residuals. The majority of the points in Figure 6a lie above the 1:1 line indicating that BC containing particles were enriched in the ice phase and that these particles preferentially acted as IN. It is observed that BC measured behind the total inlet represented between 4 to 8% of the bulk submicrometer aerosol mass, whereas the $BCMF$ of ice residuals was higher and more variable. Even though the uncertainties in $BCMF$ are relatively high (averaged over the six individual cloud events $\Delta BCMF$ is 21% for the ice particle residuals and 5% for the bulk aerosol), the determined value of the BC enrichment in ice residuals is significant.

[40] In order to confirm that the enrichment seen in Figure 6a is real (i.e., a characteristic of the ice residuals and not caused by an artifact of the instruments or inlets), the relation between the same two mass fractions ($BCMF$ in ice residual and in bulk aerosol) is also shown for all out-of-cloud periods where the CVI inlet was operated without counterflow or impactors and thus sampling both nonactivated particles and hydrometeors (Figure 6b). Here the same density was applied to both inlets ($\rho = 1.5 \text{ g cm}^{-3}$). The data points are located much closer to the 1:1 line; an orthogonal regression line through the data points has a slope of 0.85 ($r^2 = 0.38$; $BCMF_{(\text{Ice residuals})} = 0.85 \cdot BCMF_{(\text{Bulk})}$). This analysis shows that the observed enrichment is not caused by a systematic deviation induced by e.g., the calculation of ratios of values measured by different instruments.

[41] An analysis was performed to see if the variability in the enrichment could be explained by different cloud temperatures or cloud ice mass fractions, but no influence of these parameters on the observed BC enrichment was found. It was found that the variability in the $BCMF$ was predominately caused by relatively large fluctuations of $V_{\text{SMPS}(\text{Ice-CVI})}$ (while $BC_{\text{PSAP}(\text{Ice-CVI})}$ was found to be fairly constant). A hypothesis is that these fluctuations are caused by dust events which have a significant influence on the submicrometer volume (as shown in Figure 2). This hypothesis cannot be proved because no quantitative dust measurements were available.

[42] Measurements from the ATOFMS support the BC enrichment in the ice phase. Behind the total inlet during out-of-cloud conditions BC represented approximately 5% of the bulk particles by number. The concentration of BC in the ice residuals was enriched, representing, as a lower limit (see above), between 7 and 10% of the particles by number over the course of the campaign. Because the ATOFMS alternately sampled of either the Ice-CVI or total inlet an enrichment factor cannot be correctly inferred from these values. At the single particle level BC was found to be

internally mixed with organic carbon for all particles sampled (i.e., mass spectra of particles with BC always contained fragments associated with organic carbon) and often with potassium, an indicator of biomass burning [Hudson *et al.*, 2004]. Black carbon was occasionally internally mixed with other species such as mineral dust and metal oxides although, by number, this constituted less than 10% of the BC sampled.

[43] Further research, for example by means of a single particle soot photometer (Droplet Measurement Technology, SP2), to look at individual BC particles, at their size distributions in the aerosol and at their mixing state would be of major interest. In this study, we observed a distinct enrichment of BC containing particles in ice residuals in terms of mass. Preliminary results on the BC enrichment in terms of number were estimated. This important topic clearly needs further research. An open question is if the carbon aggregates in the particles are the active site for ice nucleation or if other substances associated with BC play the active role. In parallel to field studies, more laboratory measurements are required. The existing literature is often in conflict with some papers indicating very high freezing thresholds for BC whereas others are much lower. Investigations as a function of freezing mechanism (e.g., contact, immersion, and deposition) should be performed. In addition, the ice forming capacity of more representative (aged) tropospheric BC particles should be investigated.

4. Conclusions

[44] The BC mass fraction was found to be enriched in ice particle residuals obtained from small crystals when compared to the bulk aerosol particles. BC comprised about 5% of the bulk submicrometer aerosol mass whereas the mass fraction was on average 27% for the ice particle residuals. This includes data from 106 hours of in-cloud measurements. This enrichment in ice particle residuals suggests that some fraction of atmospheric BC can act as ice nuclei in mixed phase clouds. It remains uncertain what property of these BC-containing aerosols results in a higher nucleating capacity and future studies are needed to clarify this. This might have important implications for the indirect aerosol effect via glaciation of clouds. An increasing BC concentration due to anthropogenic activities is expected and, if these particles have an increased capacity to form ice, this could lead to a decrease in the lifetime of clouds by more efficiently initiating precipitation.

[45] **Acknowledgments.** We thank the International Foundation High Altitude Research Stations Jungfraujoch and Gornegrat (HFSJG) for the opportunity to perform experiments at the Jungfraujoch. This work was supported by MeteoSwiss (GAW program), as well as the German Science foundation (grants He 939/8-1,2 and He 939/17-1) and the EC project ACCENT. The analyses were partially supported by the Collaborative Research Center SFB 641 from the Deutsche Forschungsgemeinschaft.

References

- Alfaro, S. C., S. Lafon, J. L. Rajot, P. Formenti, A. Gaudichet, and M. Maille (2004), Iron oxides and light absorption by pure desert dust: An experimental study, *J. Geophys. Res.*, *109*, D08208, doi:10.1029/2003JD004374.
- Baltensperger, U., H. W. Gäggeler, D. T. Jost, M. Lugauer, M. Schwikowski, E. Weingartner, and P. Seibert (1997), Aerosol climatology at the high-alpine site Jungfraujoch, Switzerland, *J. Geophys. Res.*, *102*(D16), 19,707–19,715.

- Bond, T. C., T. L. Anderson, and D. Campbell (1999), Calibration and intercomparison of filter-based measurements of visible light absorption by aerosols, *Aerosol Sci. Technol.*, *30*(6), 582–600.
- Bond, T. C., and R. W. Bergstrom (2006), Light absorption by carbonaceous particles: An investigative review, *Aerosol Sci. Technol.*, *40*, 27–67.
- Chen, J. P., and D. Lamb (1999), Simulation of cloud microphysical and chemical processes using a multicomponent framework. part II: Microphysical evolution of a wintertime orographic cloud, *J. Atmos. Sci.*, *56*(14), 2293–2312.
- Chen, Y. L., S. M. Kreidenweis, L. M. McInnes, D. C. Rogers, and P. J. DeMott (1998), Single particle analyses of ice nucleating aerosols in the upper troposphere and lower stratosphere, *Geophys. Res. Lett.*, *25*(9), 1391–1394.
- Collaud Coen, M., E. Weingartner, S. Nyeki, J. Cozic, S. Henning, B. Verheggen, R. Gehrig, and U. Baltensperger (2007), Long-term trend analysis of aerosol variables at the high alpine site Jungfraujoch, *J. Geophys. Res.*, *112*, D13213, doi:10.1029/2006JD007995.
- Cozic, J., B. Verheggen, S. Mertes, P. Connolly, K. Bower, A. Petzold, U. Baltensperger, and E. Weingartner (2007), Scavenging of black carbon in mixed phase clouds at the high alpine site Jungfraujoch, *Atmos. Chem. Phys.*, *7*, 1797–1807.
- Cozic, J., et al. (2008), Chemical composition of free tropospheric aerosol for PM1 and coarse mode at the high alpine site Jungfraujoch, *Atmos. Chem. Phys.*, *8*, 407–423.
- Cziczo, D. J., D. M. Murphy, P. K. Hudson, and D. S. Thomson (2004), Single particle measurements of the chemical composition of cirrus ice residue during crystal-face, *J. Geophys. Res.*, *109*, D04201, doi:10.1029/2003JD004032.
- DeMott, P. J. (1990), An exploratory-study of ice nucleation by soot aerosols, *J. Appl. Meteorol.*, *29*, 1072–1079.
- DeMott, P. J. (2002), Laboratory studies of cirrus cloud processes, chap. 5, in *Cirrus*, edited by D. K. Lynch et al., Oxford Univ. Press, New York.
- DeMott, P. J., Y. Chen, S. M. Kreidenweis, D. C. Rogers, and D. E. Sherman (1999), Ice formation by black carbon particles, *Geophys. Res. Lett.*, *26*, 2429–2432.
- DeMott, P. J., D. J. Cziczo, A. J. Prenni, D. M. Murphy, S. M. Kreidenweis, D. S. Thomson, R. Borys, and D. C. Rogers (2003), Measurements of the concentration and composition of nuclei for cirrus formation, *Proc. Natl. Acad. Sci. U.S.A.*, *100*, 14,655–14,660.
- Diehl, K., and S. K. Mitra (1998), A laboratory study of the effects of a kerosene-burner exhaust on ice nucleation and the evaporation rate of ice crystals, *Atmos. Environ.*, *32*, 3145–3151.
- Dymarska, M., B. J. Murray, L. M. Sun, M. L. Eastwood, D. A. Knopf, and A. K. Bertram (2006), Deposition ice nucleation on soot at temperatures relevant for the lower troposphere, *J. Geophys. Res.*, *111*, D04204, doi:10.1029/2005JD006627.
- Finlayson-Pitts, B. J., and J. N. J. Pitts (2000), *Chemistry of the Upper and Lower Atmosphere*, Elsevier, New York.
- Fukuta, N., and T. Takahashi (1999), The growth of atmospheric ice crystals: A summary of findings in vertical supercooled cloud tunnel studies, *J. Atmos. Sci.*, *56*(12), 1963–1979.
- Fuller, K. A., W. C. Malm, and S. M. Kreidenweis (1999), Effects of mixing on extinction by carbonaceous particles, *J. Geophys. Res.*, *104*(D13), 15,941–15,954.
- Gard, E., J. E. Mayer, B. D. Morrical, T. Dienes, D. P. Fergenson, and K. A. Prather (1997), Real-time analysis of individual atmospheric aerosol particles: Design and performance of a portable ATOFMS, *Anal. Chem.*, *69*, 4083–4091.
- Gorbunov, B., A. Baklanov, N. Kakutkina, H. L. Windsor, and R. Toumi (2001), Ice nucleation on soot particles, *J. Aerosol Sci.*, *32*, 199–215.
- Heintzenberg, J. (1989), Fine particles in the global troposphere, *Tellus*, *41*, 149–160.
- Heintzenberg, J., K. Okada, and J. Strom (1996), On the composition of non-volatile material in upper tropospheric aerosols and cirrus crystals, *Atmos. Res.*, *41*, 81–88.
- Hudson, P. K., D. M. Murphy, D. J. Cziczo, D. S. Thomson, J. A. deGouw, C. Warneke, J. Holloway, J. R. Jost, and G. Hubler (2004), Biomass-burning particle measurements: Characteristic composition and chemical processing, *J. Geophys. Res.*, *109*, D23S27, doi:10.1029/2003JD004398.
- Intergovernmental Panel on Climate Change (IPCC) (2007), *Climate Change 2007: The Physical Basis of Climate Change*, IPCC Secretariat, Geneva, Switzerland. (Available at <http://www.ipcc.ch>; Working Group I, Final Report, available at <http://ipcc-wg1.ucar.edu/wg1/wg1-report.html>)
- Jayne, J. T., D. C. Leard, X. F. Zhang, P. Davidovits, K. A. Smith, C. E. Kolb, and D. R. Worsnop (2000), Development of an aerosol mass spectrometer for size and composition analysis of submicron particles, *Aerosol Sci. Technol.*, *33*(1–2), 49–70.
- Kärcher, B., O. Möhler, P. J. DeMott, S. Pechtl, and F. Yu (2007), Insights into the role of soot aerosols in cirrus cloud formation, *Atmos. Chem. Phys.*, *7*, 4203–4227.
- Krivacsy, Z., et al. (2001), Study on the chemical character of water soluble organic compounds in fine atmospheric aerosol at the Jungfraujoch, *J. Atmos. Chem.*, *39*(3), 235–259.
- Lavanchy, V. M. H., H. W. Gäggeler, S. Nyeki, and U. Baltensperger (1999), Elemental carbon (EC) and black carbon (BC) measurements with a thermal method and an aethalometer at the high-alpine research station Jungfraujoch, *Atmos. Environ.*, *33*(17), 2759–2769.
- Linke, C., O. Möhler, A. Veres, A. Mohacsi, Z. Bozoki, G. Szabo, and M. Schnaiter (2006), Optical properties and mineralogical composition of different Saharan mineral dust samples: A laboratory study, *Atmos. Chem. Phys.*, *6*, 3315–3323.
- Liu, P. S. K., et al. (2007), Transmission efficiency of an aerodynamic focusing lens system: Comparison of model calculations and laboratory measurements for the Aerodyne Aerosol Mass Spectrometer, *Aerosol Sci. Technol.*, *41*, 721–733.
- Lohmann, U. (2002), A glaciation indirect aerosol effect caused by soot aerosols, *Geophys. Res. Lett.*, *29*(4), 1052, doi:10.1029/2001GL014357.
- Lohmann, U., and K. Diehl (2006), Sensitivity studies of the importance of dust ice nuclei for the indirect aerosol effect on stratiform mixed phase clouds, *J. Atmos. Sci.*, *63*(3), 968–982.
- Mertes, S., et al. (2007), Counterflow virtual impactor based collection of small ice particles in mixed phase clouds for the physico-chemical characterisation of tropospheric ice nuclei: Sampler description and first case study, *Aerosol Sci. Technol.*, *41*, 848–864.
- Möhler, O., C. Linke, H. Saathoff, M. Schnaiter, R. Wagner, A. Mangold, M. Kramer, and U. Schurath (2005a), Ice nucleation on flame soot aerosol of different organic carbon content, *Meteorol. Z.*, *14*(4), 477–484.
- Möhler, O. M., et al. (2005b), Effect of sulfuric acid coating on heterogeneous ice nucleation by soot aerosol particles, *J. Geophys. Res.*, *110*, D11210, doi:10.1029/2004JD005169.
- Penner, J. E., M. O. Andreae, H. Annegarn, L. Barrie, J. Feichter, D. Hegg, A. Jayaraman, R. Leaitch, D. Murphy, and J. Nganga (2001), Aerosols, their direct and indirect effects, in *Climate Change 2001: The Scientific Basis—Contributions of Working Group I to the Third Assessment Report of the Intergovernmental Panel on Climate Change*, edited by J. T. Houghton et al., pp. 291–336, Cambridge Univ. Press, New York.
- Prenni, A. J., P. J. DeMott, C. Twohy, M. R. Poellot, S. M. Kreidenweis, D. C. Rogers, S. D. Brooks, M. S. Richardson, and A. J. Heymsfield (2007), Examinations of ice formation processes in Florida cumuli using ice nuclei measurements of anvil ice crystal particle residues, *J. Geophys. Res.*, *112*, D10221, doi:10.1029/2006JD007549.
- Pruppacher, H. R., and J. D. Klett (1997), *Microphysics of Clouds and Precipitation*, 2nd ed., p. 954, Kluwer Acad., Dordrecht.
- Reid, J. S., P. V. Hobbs, C. Lioussie, J. V. Martins, R. E. Weiss, and T. F. Eck (1998), Comparisons of techniques for measuring shortwave absorption and black carbon content of aerosols from biomass burning in Brazil, *J. Geophys. Res.*, *103*(D24), 32,031–32,040.
- Richardson, M. S., et al. (2007), Measurements of heterogeneous ice nuclei in the western United States in springtime and their relation to aerosol characteristics, *J. Geophys. Res.*, *112*, D02209, doi:10.1029/2006JD007500.
- Rogers, D. C., P. J. DeMott, and S. M. Kreidenweis (2001), Airborne measurements of tropospheric ice-nucleating aerosol particles in the Arctic spring, *J. Geophys. Res.*, *106*(D14), 15,053–15,063.
- Schröder, F. P., B. Kärcher, A. Petzold, R. Baumann, R. Busen, C. Hoell, and U. Schumann (1998), Ultrafine aerosol particles in aircraft plumes: In situ observations, *Geophys. Res. Lett.*, *25*(15), 2789–2792.
- Seinfeld, J. H., and S. N. Pandis (1998), *Atmospheric chemistry and physics: From air pollution to climate change*, John Wiley, New York.
- Sokolik, I. N., and O. B. Toon (1999), Incorporation of mineralogical composition into models of the radiative properties of mineral aerosol from UV to IR wavelengths, *J. Geophys. Res.*, *104*(D8), 9423–9444.
- Song, N. H., and D. Lamb (1994), Experimental Investigations of Ice in Supercooled Clouds. 2. Scavenging of an Insoluble Aerosol, *J. Atmos. Sci.*, *51*, 104–116.
- Sjogren, S., M. Gysel, E. Weingartner, M. R. Alfarra, J. Duplissy, J. Cozic, J. Crosier, H. Coe, and U. Baltensperger (2007), Hygroscopicity of the submicrometer aerosol at the high-alpine site Jungfraujoch, 3580 m a.s.l., Switzerland, *Atmos. Chem. Phys. Discuss.*, *7*, 13,699–13,732.
- Ström, J., and S. Ohlsson (1998a), In situ measurements of enhanced crystal number densities in cirrus clouds caused by aircraft exhaust, *J. Geophys. Res.*, *103*(D10), 11,355–11,361.
- Ström, J., and S. Ohlsson (1998b), Real-time measurement of absorbing material in contrail ice using a counterflow virtual impactor, *J. Geophys. Res.*, *103*(D8), 8737–8741.
- Targino, A. C., R. Krejci, K. J. Noone, and P. Glantz (2006), Single particle analysis of ice crystal residuals observed in orographic wave clouds over Scandinavia during INTACC experiment, *Atmos. Chem. Phys.*, *6*, 1977–1990.

- Tenberken Pötzsch, B., M. Schwikowski, and H. W. Gäggeler (2000), A method to sample and separate ice crystals and supercooled cloud droplets in mixed phased clouds for subsequent chemical analysis, *Atmos. Environ.*, *34*(21), 3629–3633.
- Twohy, C. H., and M. R. Poellot (2005), Chemical characteristics of ice residual nuclei in anvil cirrus clouds: Evidence for homogeneous and heterogeneous ice formation, *Atmos. Chem. Phys.*, *5*, 2289–2297.
- Verheggen, B., J. Cozic, E. Weingartner, K. Bower, S. Mertes, P. Connolly, M. Flynn, M. Gallagher, T. Choulaton, and U. Baltensperger (2007), Aerosol activation in mixed phase clouds at the high Alpine site Jungfraujoch, *J. Geophys. Res.*, *112*, D23202, doi:10.1029/2007JD008714.
- Weingartner, E., S. Nyeki, and U. Baltensperger (1999), Seasonal and diurnal variation of aerosol size distributions ($10 < D < 750$ nm) at a high-alpine site (Jungfraujoch 3580 m asl), *J. Geophys. Res.*, *104*(D21), 26,809–26,820.
- Zelenyuk, A., Y. Cai, and D. Imre (2006), From agglomerates of spheres to irregularly shaped particles: Determination of dynamic shape factors from measurements of mobility and vacuum aerodynamic diameters, *Aerosol Sci. Technol.*, *40*, 197–217.
- U. Baltensperger and E. Weingartner, Laboratory of Atmospheric Chemistry, Paul Scherrer Institut, CH-5232 Villigen PSI, Switzerland. (ernest.weingartner@psi.ch)
- J. Cozic, NOAA, Earth System Research Laboratory, 325 Broadway R/CSD2, Boulder, CO 80305-3337, USA.
- D. J. Cziczo, Pacific Northwest National Laboratory, Atmospheric Science and Global Change Division, MSIN K9-24, Richland, WA 99354, USA.
- S. J. Gallavardin, Institute for Atmospheric and Climate Science, ETH Zürich, Universitätsstrasse 16, CH-8093 Zürich, Switzerland.
- S. Mertes, Leibniz Institute for Tropospheric Research, Permoserstrasse 15, D-04318, Leipzig, Germany.
- B. Verheggen, Department of Air Quality and Climate Change, Energy Research Centre of the Netherlands ECN, P.O. Box 1, 1755 ZG Petten, Netherlands.
- S. Walter, Particle Chemistry Department, Max Planck Institute for Chemistry, Joh.-J.-Becherweg 27, D-55128, Mainz, Germany.